electricity

MDPI

Article

Adaptive Dynamic Binary Whale Optimization Algorithm for Optimal Distribution Network Reconfiguration

Americo Guerrero Poma [1], Dionicio Zocimo Ñaupari Huatuco [1,*], Yuri Percy Molina Rodriguez [2], Franklin Jesus Simeon Pucuhuayla [1], Jefferson Leandro do Nascimento [2] and Juan Pablo Bautista Rios [1]

[1] Facultad de Ingeniería Eléctrica y Electrónica, Universidad Nacional de Ingeniería, Av. Túpac Amaru 210, Rímac, Lima 15333, Peru; aguerrerop@uni.pe (A.G.P.); franklin.simeon.p@uni.pe (F.J.S.P.); jbautista@uni.edu.pe (J.P.B.R.)
[2] Department of Electrical Engineering, Federal University of Paraíba, João Pessoa 58051-900, Brazil; molina.rodriguez@cear.ufpb.br (Y.P.M.R.); jefferson.donascimento@estudante.cear.ufpb.br (J.L.d.N.)
* Correspondence: znaupari@uni.edu.pe

Abstract

This paper proposes an Adaptive Dynamic Binary Whale Optimization Algorithm (AD-BWOA) for solving the Distribution Network Reconfiguration (DNR) problem. The proposed method combines a nonlinear adaptation of the convergence parameter, a hybrid deterministic–stochastic mechanism for position-update selection, a binary transfer strategy, and a stagnation-based stopping criterion to improve the balance between exploration and exploitation and reduce unnecessary search iterations. The algorithm is implemented in Python and integrated with DIgSILENT PowerFactory, which performs the load-flow calculations and verifies the operational constraints of each candidate configuration. The performance of AD-BWOA is evaluated on 69-, 94-, and 135-bus distribution systems through 100 independent runs. The results show that the proposed method consistently reaches the best or reference solutions reported for the evaluated systems, with high repeatability in the 69- and 94-bus cases and competitive performance in the 135-bus system. In addition, the adaptive mechanisms contribute to reducing the number of iterations required for convergence under the adopted stopping criteria. The results indicate that AD-BWOA is a promising and reliable approach for discrete DNR problems, particularly when search-space reduction and adaptive control mechanisms are combined.

Keywords: distribution network reconfiguration; power loss reduction; whale optimization algorithm; metaheuristic optimization; adaptive optimization; electrical distribution systems

Check for updates

Academic Editor: Andreas Sumper

Received: 22 August 2026
Revised: 23 October 2026
Accepted: 25 October 2026
Published: 3 November 2026

Copyright: © 2026 by the authors. Licensee MDPI, Basel, Switzerland. This article is an open access article distributed under the terms and conditions of the Creative Commons Attribution (CC BY) license.

1. Introduction

The reduction of power losses in electrical distribution systems has become one of the main research challenges in modern power systems due to its direct impact on operational efficiency and energy savings. Traditionally, several strategies have been adopted to mitigate these losses, including the installation of capacitor banks and the integration of distributed generation (DG). However, Distribution Network Reconfiguration (DNR) has emerged as a more efficient alternative because it enables the reduction of line losses without requiring additional investment in new equipment [1]. DNR modifies the network topology through the coordinated opening and closing of sectionalizing and tie switches while maintaining system radiality and satisfying operational constraints. These modifications directly influence power flow distribution and significantly affect the overall level of energy losses in the network.

Due to the combinatorial and non-linear nature of the DNR problem, numerous metaheuristic optimization approaches have been proposed in the literature. Pegado et al. [2] introduced the Improved Selective Binary Particle Swarm Optimization (IS-BPSO), which incorporates a control parameter in the sigmoidal transfer function to enhance stability and convergence performance, achieving significant power loss reductions in 33- and 94-bus systems. Nguyen et al. [3] proposed the Enhanced Binary Cuckoo Search Algorithm (EBCSA), which adapts the cuckoo search method to the binary domain and integrates a local search mechanism, demonstrating superior performance compared to several benchmark algorithms in systems with up to 136 buses. Similarly, Kahouli et al. [4] investigated loss reduction and reliability improvement using techniques such as exhaustive search, genetic algorithms, and PSO, highlighting the latter for its computational efficiency.

In recent years, several nature-inspired metaheuristic algorithms have also been explored to address the DNR problem. Solanki et al. [5] applied the Whale Optimization Algorithm (WOA), obtaining power loss reductions of 31.1% and 55.58% in 33- and 69-bus systems, respectively. Alqahtani et al. [6] implemented the Gray Wolf Optimization (GWO) algorithm, achieving improvements of up to 56.44% in power loss reduction. Wu et al. [7] developed a hybrid Chaos PSO–Chicken Swarm Fusion Optimization (CPSCSFO) algorithm that integrates chaotic mechanisms and encoding strategies to guarantee valid radial configurations, achieving reductions of up to 69.59% when distributed generation is considered. Likewise, Siregar et al. [8] confirmed the superiority of PSO over exhaustive search techniques, while Jia et al. [9] proposed the Improved Arithmetic Optimization Algorithm (IAOA), incorporating diversification strategies and adaptive control mechanisms to enhance convergence and avoid local optima. More recently, Dehghany and Asghari [1] introduced a multi-objective approach based on the Wild Mice Colony (WMC) algorithm, simultaneously optimizing power losses, voltage profile, and reliability, obtaining superior results compared to conventional methods.

Despite the significant progress reported in the literature, many existing methods still suffer from premature convergence or stagnation in local optima when dealing with large and complex distribution systems. Therefore, there is a need for more robust optimization frameworks capable of maintaining a suitable balance between exploration and exploitation during the search process.

Table 1 summarizes the main studies reported in the literature, highlighting the year of publication, optimization method, test system, and source of publication for each contribution.

Recent studies indicate that metaheuristic optimization strategies, particularly those based on hybrid models and adaptive mechanisms, have shown promising results for solving the DNR problem. Multi-objective optimization frameworks that simultaneously address power loss minimization, voltage profile improvement, load balancing, and switching operation efficiency have benefited from approaches such as neural-based models (QOC-NNA), hybrid optimization schemes (FWA-IGBA), and fuzzy logic integrated with evolutionary strategies. Furthermore, the increasing penetration of renewable energy sources and electric vehicles has significantly increased the operational complexity of distribution networks, requiring more robust, flexible, and computationally efficient optimization methods.

WOA was selected as the baseline algorithm because its search dynamics are governed by a compact set of interpretable mechanisms—encircling, spiral motion, and random-agent search—whose relative activation can be directly influenced through the parameters a, A, and p. In addition, WOA has previously been applied to discrete distribution network reconfiguration, providing a relevant baseline for evaluating WOA-specific adaptive and binary/discrete extensions. Therefore, the selection of WOA does not imply that it is universally superior to other metaheuristic approaches; rather, it provides an established

framework in which the proposed convergence-control, position-update selection, and stopping mechanisms can be systematically evaluated for the combinatorial DNR problem.

Table 1. Summary of the reviewed literature on distribution network reconfiguration.

Ref.	Year	Method/Algorithm	Test System	Source
[2]	2019	Improved Selective Binary Particle Swarm Optimization (IS-BPSO)	33-bus, 94-bus	Article
[3]	2021	Enhanced Binary Cuckoo Search Algorithm (EBCSA)	33-bus, 69-bus, 70-bus, 136-bus	Article
[4]	2021	Exhaustive Search, Genetic Algorithm and PSO with BIBC-BCBV Load Flow	33-bus	Article
[5]	2023	Whale Optimization Algorithm (WOA) for Discrete DNR	33-bus, 69-bus	Article
[6]	2023	Gray Wolf Optimization (GWO) for Distribution Network Reconfiguration	33-bus, 69-bus	Article
[7]	2023	Hybrid Chaos PSO–Chicken Swarm Fusion Optimization (CPSCSFO)	33-bus	Article
[8]	2024	Exhaustive Search and Particle Swarm Optimization (PSO)	33-bus	Article
[9]	2024	Improved Arithmetic Optimization Algorithm (IAOA)	33-bus, 69-bus	Article
[1]	2024	Multi-objective Wild Mice Colony (WMC) Algorithm	33-bus, 69-bus	Article

Within this framework, this research introduces a novel approach based on the Adaptive Dynamic Binary Whale Optimization Algorithm (AD-BWOA). The proposed algorithm extends the conventional Whale Optimization Algorithm by incorporating adaptive updating mechanisms designed to improve convergence behavior and prevent stagnation in local optima. The model integrates dynamic control parameters, binary transfer functions, and operators inspired by the cooperative hunting behavior of humpback whales, which are specifically adapted to address discrete decision problems such as distribution network reconfiguration.

The main contributions of this work can be summarized as follows:

(a) An adaptive dynamic binary optimization framework based on the Whale Optimization Algorithm (WOA) is developed for the Distribution Network Reconfiguration (DNR) problem, integrating adaptive search control, discrete decision mechanisms, and feasibility verification within a unified solution procedure.
(b) A nonlinear formulation of the convergence parameter a, based on the combination of the conventional linear decay and an exponential modulation term, is incorporated to provide a dynamic evolution of the search intensity throughout the optimization process.
(c) A hybrid deterministic–stochastic formulation of the parameter p is integrated with the nonlinear evolution of a, allowing the probability of selecting the position-update mechanism to vary according to the convergence state of the algorithm while preserving a stochastic search component.
(d) A fundamental-loop-based search-space reduction strategy and a binary transfer mechanism are incorporated to adapt the continuous WOA search dynamics to the discrete and combinatorial nature of DNR while enforcing radiality, connectivity, and electrical operating constraints.
(e) A stagnation-based stopping criterion is introduced to terminate the search when no further improvement in the best solution is observed over a predefined number of

consecutive iterations, thereby avoiding unnecessary iterations under the adopted computational framework.

(f) The proposed AD-BWOA is evaluated through multiple independent runs on 69-, 94-, and 135-bus distribution systems. The results show high repeatability in the 69- and 94-bus cases and competitive solution quality for the larger 135-bus system when compared with reference results reported in the literature.

This paper is organized as follows. Section 2 presents the Distribution Network Reconfiguration (DNR) problem formulation. Section 3 describes the fundamental principles of the Whale Optimization Algorithm (WOA). Section 4 introduces the proposed method, referred to as AD-BWOA, together with its adaptive mechanisms. Section 5 presents the application of the AD-BWOA algorithm to the distribution network reconfiguration problem. Subsequently, Section 6 provides the simulation results and the corresponding analysis. Finally, Section 7 summarizes the main conclusions of this study.

2. Distribution Network Reconfiguration (DNR)

Distribution network reconfiguration is a nonlinear and combinatorial problem whose objective is to determine the optimal status of sectionalizing and tie switches in order to reduce active power losses, balance loads, improve the voltage profile, and enhance system reliability [10]. The configuration is modeled using binary variables (open/closed), considering only the switches associated with fundamental loops in order to reduce the search space without compromising solution quality.

Switching operations modify the network topology; therefore, it is essential to guarantee radiality, service continuity, and compliance with operational constraints. From a graph theory perspective, the network must maintain a radial structure equivalent to a spanning tree, ensuring full connectivity while avoiding the formation of electrical islands [11].

The main objective of DNR is to minimize active power losses in distribution lines [10], which can be expressed as:

$$\min \sum_{b=1}^{N_b} I_b^2 R_b \tag{1}$$

where

- b: Branch index;
- N_b: Total number of branches;
- I_b: Current flowing through branch b;
- R_b: Resistance of branch b;
- min $\sum$: Total active power losses (kW).

During system operation, several constraints must be satisfied, which are described as follows.

- Radiality constraint: The distribution system must operate in a radial configuration, meaning that closed loops are not allowed in the network. Consequently, the total number of branches is determined by the following expression:

$$N_{branch} = N_{buses} - 1 \tag{2}$$

where N represents the total number of buses.

$$N_{\text{loops}} = N_{\text{inter}} - N_{\text{branch}} \tag{3}$$

where N_{loops} denotes the number of independent loops in the network, N_{inter} represents the total number of interconnections (including tie lines), and N_{branch} corresponds to the number of branches required for radial operation.

- Voltage constraint: At each bus, the voltage magnitude must satisfy the following condition:

$$V_{\min} \leq V_i \leq V_{\max} \tag{4}$$

where $V_{\min} = 0.95$ p.u. and $V_{\max} = 1.05$ p.u. represent the lower and upper voltage limits at bus i.

- Current constraint: The magnitude of the current in each branch must satisfy:

$$I_b < I_b^{\max} \tag{5}$$

where $I_b^{\max}$ is the maximum allowable current in branch b.

- Feasibility constraint: It is ensured that no load becomes isolated during the reconfiguration process.

3. Whale Optimization Algorithm (WOA)

Humpback whales are marine mammals known for a distinctive hunting strategy called bubble-net feeding. This technique consists of generating circular or spiral-shaped bubbles to concentrate schools of small fish and krill near the surface. The hunting process occurs in three main phases: encircling the prey, the spiral bubble-net formation, and the subsequent capture of food. Each of these stages is described below [12]:

3.1. Encircling the Prey

Humpback whales identify the location of the prey as an initial position $\vec{X}(t)$ and encircle it under the assumption that the current best solution represents the target prey. Since the optimal location is unknown, the WOA assumes that the currently selected solution corresponds to the optimal one. Once the best search agent is identified, the remaining agents update their positions according to Equations (8) and (9) [12].

$$\vec{D} = \left| \vec{C} \cdot \vec{X}_b(t) - \vec{X}(t) \right| \tag{6}$$

$$\vec{X}(t+1) = \vec{X}_b(t) - \vec{A} \cdot \vec{D} \tag{7}$$

where $\vec{X}_b(t)$ is updated at each iteration. The vectors $\vec{A}$ and $\vec{C}$ are defined as follows [12]:

$$\vec{a} = 2 - \frac{2t}{T} \tag{8}$$

$$\vec{A} = 2\vec{a} \cdot \vec{r} - \vec{a} \tag{9}$$

$$\vec{C} = 2 \cdot \vec{r} \tag{10}$$

where

- t: Current generation;
- $\vec{X}_b(t)$: The best solution found so far;
- $\vec{a}$: Decreases linearly from 2 to 0;
- $\vec{r}$: Random vector in the range $[0, 1]$.

3.2. Bubble-Net Spiral Feeding Mechanism

Two strategies are considered to model the bubble-net feeding behavior of humpback whales:

(a) Shrinking encircling mechanism: This mechanism is implemented by gradually decreasing the magnitude of the parameter $\vec{a}$, thereby reducing the range of $\vec{A}$ and contracting the search region around the best solution found so far [12]. During the exploitation (hunting) phase ($|\vec{A}| \leq 1$), search agents update their positions within this shrinking region. Figure 1 illustrates the relationship between the mathematical

formulation and the resulting movement of the agents. In panel (a), the central magenta/red point (X, Y) denotes the best solution found so far, corresponding to the prey position. The colored squares (orange, blue, green, and pink) delineate concentric search regions that contract as A decreases through the values 1, 0.8, 0.5, 0.4, and 0.2. Filled colored points (blue, green, and pink) mark the initial search-agent positions associated with different values of A, whereas open circles (pink and white) indicate possible updated positions within the corresponding search regions.

(b) Spiral updating position: In this strategy, a spiral equation is used to model the helix-shaped movement of humpback whales when approaching their prey. The position of each whale is updated according to Equation (11):

$$\vec{X}(t+1) = \vec{D}' \cdot e^{bl} \cdot \cos(2\pi l) + \vec{X}_b(t) \tag{11}$$

where $\vec{D}' = \left|\vec{X}_b(t) - \vec{X}(t)\right|$ denotes the componentwise absolute difference between the current search-agent position and the best solution $\vec{X}_b(t)$, b is a constant that defines the shape of the logarithmic spiral, and l is a random number in $[-1, 1]$. Figure 1 illustrates the geometric interpretation of this update mechanism. In panel (b), the gray spiral depicts the logarithmic spiral path, and the gray circles mark possible updated positions along it. The magenta point (X, Y) denotes the whale's current position, while the central red point (X^*, Y^*) denotes the best solution found so far, corresponding to the prey position. The blue projection lines and coordinate axes illustrate how l determines the exponential scaling and cosine modulation in Equation (11), thereby defining the whale's updated position relative to the prey.

Whales swim around the prey with a probability $p = 0.5$ to choose between the shrinking encircling mechanism or the spiral model. This behavior is mathematically expressed in Equation (12) [12]:

$$\vec{X}(t+1) = \begin{cases} \vec{X}_b(t) - \vec{A} \cdot \vec{D}, & \text{si } p < 0.5, \\ \vec{D}' \cdot e^{bl} \cdot \cos(2\pi l) + \vec{X}_b(t), & \text{si } p \geq 0.5. \end{cases} \tag{12}$$

where

- p: Random number in the range $[0, 1]$;
- l: Random number in the range $[-1, 1]$;
- b: Parameter that defines the shape of the logarithmic spiral.

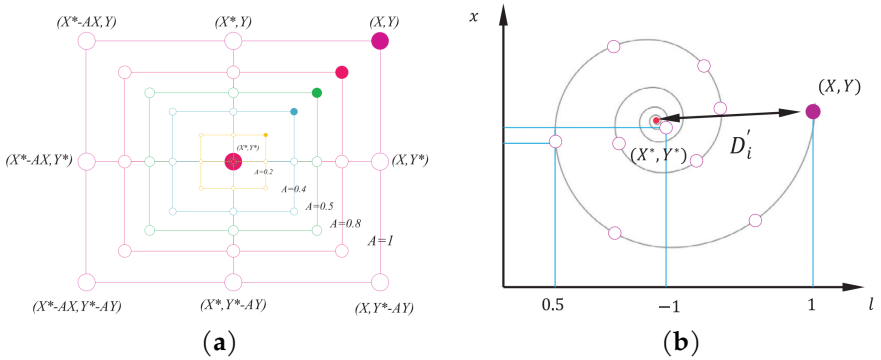


Figure 1. Illustration of the WOA mechanisms: (**a**) prey searching and (**b**) spiral updating position.

3.3. Prey Searching

Instead of using $\vec{X}_b(t)$, a random candidate solution $\vec{X}_{rand}(t)$ is selected. This allows the WOA to move the agents away from the reference whale. By imposing $|\vec{A}| > 1$, the exploration phase enables global search. The equations are presented below (13) and (14):

$$\vec{D} = \left|\vec{C} \cdot \vec{X}_{rand}(t) - \vec{X}(t)\right| \tag{13}$$

To properly interpret the relationship between the equation and the trajectory, see Figure 2.

$$\vec{X}(t+1) = \vec{X}_{rand}(t) - \vec{A} \cdot \vec{D} \tag{14}$$

where $\vec{X}_{rand}$ is a random position vector from the current population.

Figure 2 illustrates the global exploration mechanism. The central magenta point surrounded by colored rings denotes a randomly selected whale, $\vec{X}_{rand}(t)$, which serves as the reference position for updating the search agents. The colored squares (pink, green, blue, and orange) delineate search regions that expand as A increases through the values 1, 1.4, 1.5, 1.8, and 2. This expansion illustrates how $\vec{A}$ controls the extent of agent displacement relative to the selected whale, enabling a broader search of the solution space and promoting global exploration.

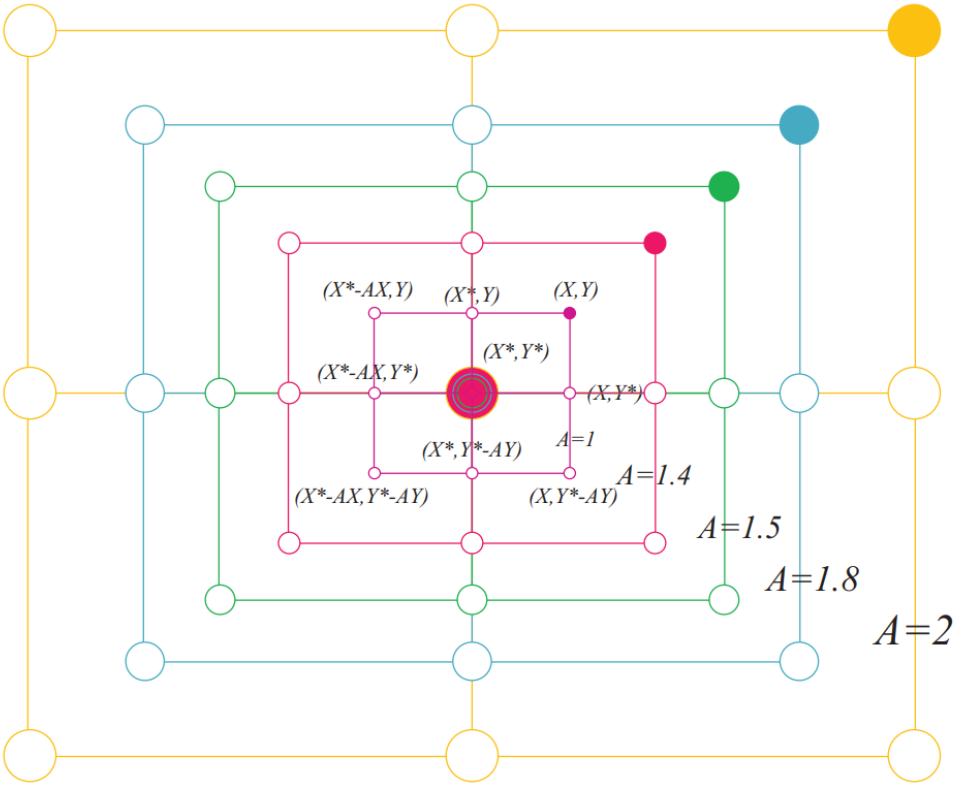


Figure 2. Prey-searching mechanism of the WOA.

4. Proposed Method—(AD-BWOA)

A strategy based on the Whale Optimization Algorithm (WOA) is proposed, incorporating a dynamic control scheme for the key parameter a and a binary decision mechanism in order to reinforce the balance between global exploration and local exploitation. The approach progressively reduces the magnitude of changes throughout the iterations, starting with a broad exploration phase and evolving toward a fine-tuning of the solutions. This adaptation improves stability, search efficiency, and performance in non-convex and multimodal spaces, which are characteristic of distribution network reconfiguration problems.

The implementation is developed in Python 3.13., using DIgSILENT PowerFactory 2024 through its API as the computational engine. Python manages the optimization logic and generates candidate solutions, while PowerFactory performs the load-flow analysis

and returns electrical variables such as voltages, currents, and power losses, forming an integrated evaluation environment.

4.1. Modification of Parameter a in the WOA Algorithm

In the original WOA, the control parameter a decreases linearly over iterations, as defined in Equation (8). This parameter controls the magnitude of the coefficient vector $\vec{A}$ and, consequently, influences the transition between exploration and exploitation during the optimization process

Several improved WOA variants have modified the conventional linear evolution of (a) using nonlinear strategies. For example, Sun et al. [13] introduced a nonlinear decreasing strategy for the convergence factor to regulate the exploration–exploitation process according to the iteration number. Therefore, the use of a nonlinear convergence factor is not considered an independent novelty of the present work. In the proposed AD-BWOA, a specific nonlinear formulation is adopted by combining the conventional linear decay of (a) with an exponential modulation factor. First, the exponential factor is defined as

$$\delta = e^{-k\frac{t}{\max_{\text{iter}}}}, \tag{15}$$

where $k > 0$ is a control parameter that determines the intensity of the exponential modulation, (t) denotes the current iteration, and max_{iter} represents the maximum number of iterations. The convergence parameter is then calculated as

$$a = 2\left(1 - \frac{t}{\max_{\text{iter}}}\right)\delta, \tag{16}$$

This formulation preserves the decreasing behavior of the conventional WOA parameter while introducing an additional exponential modulation controlled by k. Consequently, the evolution of a is determined jointly by the iteration-dependent linear term and the exponential factor, providing a nonlinear variation of the search intensity throughout the optimization process. The role of this formulation in the proposed AD-BWOA is not to claim nonlinear adaptation of a as an isolated contribution, since similar strategies have previously been reported in the WOA literature. Instead, a provides the adaptive state used by the subsequent hybrid formulation of the whale position mechanism p, establishing a direct relationship between the convergence state of the algorithm and the selection of the position-update mechanism. Thus, in the proposed framework, the evolution of a constitutes one component of the coordinated adaptive mechanism described in the following subsection.

4.2. Adaptive Determination of the Whale Position Mechanism p

In the standard WOA, the parameter p is randomly generated within the interval $[0, 1]$, and it controls the selection between the shrinking encircling mechanism and the spiral updating strategy. In previous work by the authors, a hybrid formulation of p was developed by incorporating the convergence parameter a with a stochastic component. In the present study, this formulation is adopted and integrated with the nonlinear adaptation of (a) within the proposed AD-BWOA.

To overcome this limitation, the parameter p is redefined as a function of the control parameter a, incorporating both adaptive and stochastic components:

$$p = \alpha\left(\frac{a}{2}\right) + (1 - \alpha)\ \text{rand}(0, 1), \tag{17}$$

where $\alpha \in [0, 1]$ is a weighting factor that determines the contribution of the adaptive and stochastic components.

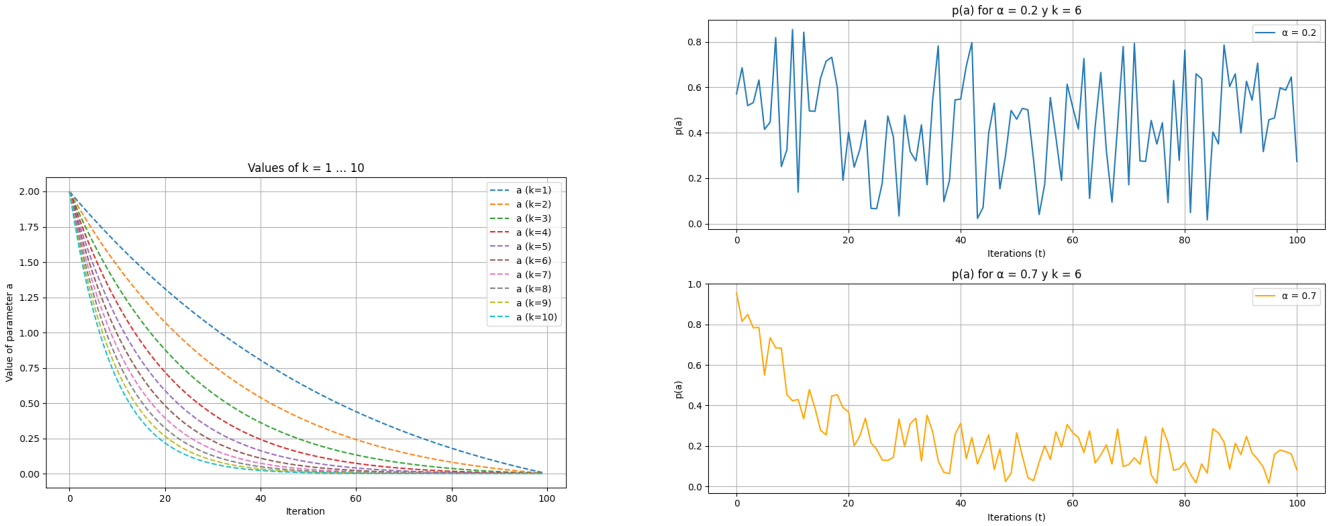
The value of p determines the position-update mechanism according to the following rule: $p < 0.5$ selects the shrinking encircling mechanism, whereas $p \geq 0.5$ selects the spiral

updating strategy. Therefore, the evolution of p directly modifies the probability of selecting each position-update mechanism during the optimization process.

Unlike the conventional random formulation, p is dynamically related to the evolution of a. Thus, the probability used to select the position-update mechanism changes according to the convergence state of the algorithm while retaining a stochastic component. This relationship allows the position-update mechanism to evolve throughout the optimization process rather than being determined exclusively by an independent random variable.

In the proposed AD-BWOA, the hybrid p is combined with the nonlinear evolution of a and the binary position-update mechanism used to determine the switching states of the distribution network. Therefore, the hybrid formulation of p is not claimed as an independent novelty of the present work. Its role in this study is to contribute to the coordinated adaptive structure of the AD-BWOA, together with the nonlinear a formulation and the stagnation-based stopping criterion.

The resulting evolution of parameters a and p throughout the optimization process is illustrated in Figure 3.



(**a**) Adaptive behavior of parameter a. (**b**) Dynamic behavior of parameter p.

Figure 3. (**a**) Evolution of parameter a and (**b**) adaptive behavior of the proposed parameter p.

4.3. Search-Space Reduction via Selective Mesh Representation

The number of possible switching configurations of a distribution network grows exponentially with the number of controllable switching elements. If n_s switches are independently represented by binary open/closed states, the unrestricted search space contains up to 2^{n_s} possible configurations. However, only a subset of these configurations satisfies the radiality and connectivity requirements of distribution network operation. Consequently, directly exploring the complete binary search space becomes increasingly inefficient as the network size and number of switching devices increase.

To reduce this search space while maintaining radial operation, the proposed method employs the concept of fundamental loops, following approaches reported in distribution system reconfiguration studies [14–17]. For an initially radial distribution network, the number of fundamental loops is determined according to

$$M = n - b, \tag{18}$$

where M represents the number of fundamental loops, n is the total number of switching elements, and b is the number of branches.

The switches associated with the identified loops are organized into specific sets. Each switching element is considered only once during the construction of the loop sets, avoiding duplicated decision variables. For each loop k, the position of the switch to be opened is selected within the valid range according to

$$j_k = \text{randi}(1, N_k), \tag{19}$$

where j_k represents the selected position of the open switch in loop k, and N_k is the number of switching elements associated with that loop.

Thus, one switch is selected as open within each fundamental loop to construct the candidate switching configuration. This representation restricts the optimization process to the switching alternatives associated with the identified loops rather than independently exploring all possible switch combinations.

When network elements are shared between loops, the corresponding switching element is treated as a single physical component and is not duplicated in the search representation. The complete switching configuration is subsequently evaluated to ensure radiality and connectivity. Configurations that produce closed cycles, disconnected buses, isolated loads, or violations of the operating constraints are considered infeasible and discarded [18].

4.4. Stopping Criteria

The AD-BWOA incorporates two complementary stopping criteria to ensure both computational efficiency and solution quality.

The first criterion defines a maximum number of iterations, denoted as N_{iter}, which limits the computational effort and ensures fair comparison with other optimization methods.

The second criterion is based on the stagnation of the search process. Specifically, the algorithm is terminated if no improvement in the global best solution ($Gbest$) is observed over a predefined number of consecutive iterations, denoted as NR_m.

Formally, the stopping condition can be expressed as:

$$\text{Stop if } (t \geq N_{iter}) \quad \text{or} \quad (\Delta Gbest = 0 \text{ for } NR_m \text{ consecutive iterations})$$

The combination of these criteria prevents unnecessary evaluations once the search process stabilizes, reduces computational overhead, and ensures that the algorithm does not continue exploring without meaningful improvements.

4.5. Binary Transfer Mechanism

Since the original WOA operates in a continuous search space, a binary transfer mechanism is required to adapt the optimization process to the discrete nature of the distribution network reconfiguration problem. It is important, however, to distinguish the internal search representation from the physical switching configuration. AD-BWOA internally updates continuous real-valued search variables, which are subsequently discretized within the admissible switching alternatives defined by the fundamental-loop representation. The resulting physical network topology is then expressed as a binary switch-state vector, where 1 denotes a closed switch and 0 denotes an open switch.

To perform this discretization, the continuous positions generated by the whales are mapped into binary switching states using a sigmoid transfer function. The sigmoid function converts each continuous position x into a scalar value within the interval $(0, 1)$, as defined in Equation (20):

$$S(x) = \frac{1}{1 + e^{-x}}. \tag{20}$$

To reduce premature stagnation and promote population diversity, a Gaussian random perturbation is introduced into the transfer process, as defined in Equation (21):

$$S'(x) = S(x) + \epsilon, \tag{21}$$

where ϵ represents the Gaussian perturbation term.

The final binary state of each decision variable is obtained by comparing the perturbed transfer value with a uniformly distributed random number $r \in [0, 1]$:

$$X_i = \begin{cases} 1, & S'(x_i) > r, \\ 0, & S'(x_i) \leq r. \end{cases} \tag{22}$$

In the distribution network reconfiguration problem, the binary value represents the switching state, where 1 denotes a closed switch and 0 denotes an open switch. The resulting binary variables define a candidate switching configuration, which is subsequently evaluated for radiality, connectivity, and electrical operating constraints through the load-flow calculation in DIgSILENT PowerFactory. No explicit feasibility-repair operator is employed in the present implementation. Instead, infeasible configurations are identified during the topological and electrical feasibility-verification stages and are rejected without updating the current best feasible solution.

This mechanism enables the continuous positions generated by AD-BWOA to be mapped into discrete switching configurations while introducing a stochastic component that helps preserve population diversity during the optimization process.

5. Application of AD-BWOA to Distribution Network Reconfiguration (DNR)

The proposed Adaptive Dynamic Binary Whale Optimization Algorithm (AD-BWOA) is applied to the Distribution Network Reconfiguration (DNR) problem, whose objective is to minimize total active power losses while maintaining the electrical and topological conditions required for network operation. The distribution network is represented by a graph $G = (V, E)$, where $V = \{1, \ldots, N_b\}$ denotes the set of buses and $E = \{1, \ldots, N_l\}$ the set of branches. A feasible radial configuration must maintain a connected and acyclic topology.

The operating states of the branches are represented by the binary vector

$$\mathbf{k} = [k_1, k_2, \ldots, k_{N_l}], \qquad k_b \in \{0, 1\}, \tag{23}$$

where $k_b = 1$ indicates that branch b remains energized and $k_b = 0$ indicates that it is open. For a given configuration $\mathbf{k}$, the energized branches define the network topology and, consequently, the electrical state obtained from the power-flow calculation.

The objective function of the DNR problem is to minimize the total active power losses in the energized branches, expressed as

$$\min_{\mathbf{k}} \quad P_{\text{loss}}(\mathbf{k}) = \sum_{b=1}^{N_l} k_b |I_b|^2 R_b, \tag{24}$$

where I_b and R_b represent the current magnitude and resistance of branch b, respectively. The term k_b considers only the branches that remain energized in the evaluated configuration.

The candidate configuration must satisfy the electrical constraints associated with voltage and current limits. For each bus,

$$V_{i,\min} \leq V_i \leq V_{i,\max}, \qquad i = 1, \ldots, N_b, \tag{25}$$

while the current in each branch must satisfy

$$|I_b| \leq I_{b,\max}, \qquad b = 1, \ldots, N_l. \tag{26}$$

For each switching configuration, the electrical variables must satisfy the power-flow equations corresponding to the evaluated topology. These conditions are compactly represented as

$$g_I(I, V, \mathbf{k}) = 0, \tag{27}$$

$$g_V(V, I, \mathbf{k}) = 0, \tag{28}$$

where g_I represents the current balance at the buses and g_V represents the voltage–current relationships of the energized branches. In the proposed implementation, these equations are solved using the DIgSILENT PowerFactory power-flow calculation for each candidate configuration. Therefore, the losses, voltages, and currents used by the algorithm correspond to the electrical state calculated for the evaluated topology.

From a topological perspective, the distribution network must maintain a radial operating structure in which each energized load bus is supplied through a unique path from the source. Therefore, a feasible configuration must be connected and must not contain closed loops. For a connected network with N_b buses and a single source, a radial configuration contains exactly $N_b - 1$ energized branches. Accordingly,

$$\sum_{b=1}^{N_l} k_b = N_b - 1. \tag{29}$$

For a connected graph, the number of independent cycles, associated with the cyclomatic number of the network, is given by

$$N_{\text{loop}} = N_l - N_b + 1, \tag{30}$$

where N_l denotes the total number of available branches and N_b the number of buses. This relationship identifies the number of independent loops in the network topology. In a radial configuration, the energized branches must form a connected and acyclic graph and, therefore, the energized topology must not contain independent cycles. For a connected network, this condition is equivalent to having $N_b - 1$ energized branches. However, satisfying this condition alone does not guarantee radiality, since a configuration with $N_b - 1$ energized branches may contain disconnected components. Therefore, topological feasibility requires both network connectivity and the absence of closed loops, ensuring that all load buses remain connected and energized from the source.

The Selective Space Mesh (SSM) incorporates the fundamental-loop information into the search process by restricting the switching variables to the elements associated with these loops. This reduces the effective search space and concentrates the reconfiguration operations on topologically relevant alternatives. Candidate configurations are subsequently verified in DIgSILENT PowerFactory to ensure compliance with connectivity, radiality, and electrical operating conditions.

The set of electrically and topologically feasible configurations can be expressed as

$$\Omega_{\text{feas}} = \left\{ \mathbf{k} \in \{0,1\}^{N_l} \;\middle|\; \begin{array}{l} g_I(I, V, \mathbf{k}) = 0, \\ g_V(V, I, \mathbf{k}) = 0, \\ V_{i,\min} \le V_i \le V_{i,\max}, \\ |I_b| \le I_{b,\max}, \\ \sum_{b=1}^{N_l} k_b = N_b - 1, \\ \text{connected and acyclic network} \end{array} \right\}. \tag{31}$$

Accordingly, the distribution network reconfiguration problem can be formulated as

$$\min_{\mathbf{k} \in \Omega_{\text{feas}}} P_{\text{loss}}(\mathbf{k}) \tag{32}$$

The AD-BWOA explores the solution space using binary search and the representation based on fundamental loops. The decision variables are restricted to the switching elements associated with these loops, reducing the effective search space. The continuous positions generated by the algorithm are transformed into binary states using the transfer mechanism defined previously.

For each candidate configuration, the switching states are transferred from Python to DIgSILENT PowerFactory, where the network topology is updated and the power-flow calculation is executed. The calculated active power losses, bus voltages, and branch currents are returned to Python to evaluate the objective function and verify the electrical and topological constraints. Infeasible configurations are discarded.

Python manages the generation and evaluation of the configurations, while DIgSILENT PowerFactory performs the electrical calculations. The iterative process continues until the maximum number of iterations is reached or the stopping criterion based on consecutive iterations without improvement in the objective function is satisfied.

The complete implementation of AD-BWOA for distribution network reconfiguration is summarized in the following steps:

1. Initial parameters. The initial conditions of the electrical system are defined using the initial feasible radial network topology and its corresponding operating conditions, including the base power, bus voltages, line currents, and network connectivity. The algorithm parameters are then defined: the whale population size (m), the upper bound of the adaptive parameter (a), the maximum number of iterations (N_{iter}), and the maximum number of consecutive iterations without improvement (NR_m).
2. Identification of fundamental loops. The fundamental loops of the meshed network are identified from the initial radial topology, enabling the construction of the constrained solution space (S_n). The number of independent loops defines the problem dimensionality (d_n). The switching elements associated with each loop are organized into specific sets, and each switching element is considered only once during the construction of these sets to avoid duplicated decision variables.
3. Initialization of positions. The whales are randomly initialized within the constrained space S_n. For each whale, one switching element is selected from each fundamental-loop set to construct an initial candidate topology. The resulting configuration is evaluated to verify radiality and connectivity before performing the electrical evaluation. The initial individual best solutions (P_{best}) are assigned, and the best feasible solution found by the population (G_{best}) is determined.
4. Iterative condition. The optimization process starts and continues while $t < N_{iter}$ and no stagnation condition is met, i.e., no improvement in the best feasible objective value (P_{best}) is observed for NR_m consecutive iterations.
5. Evaluation and update of P_{best}. Each new topological configuration is evaluated through the binarization process and topological feasibility verification. The corresponding switching states are transferred from Python to DIgSILENT PowerFactory, where the load flow is executed. The resulting branch currents, bus voltages, and active power losses are returned to Python for evaluation of the objective function and operating constraints. Configurations that violate radiality, connectivity, voltage, current, or other specified operating constraints are considered infeasible. If $f(X_i) < Pbest_i$ for a feasible configuration, the individual best value of the whale is updated; otherwise, the previous value is retained.
6. Adaptive parameter a. The parameter a regulates the search behavior throughout the optimization process. In this version of AD-BWOA, it is adjusted according to the nonlinear formulation presented in Equation (16), allowing the search behavior to change progressively during the iterations.

7. Update of movement parameters. The parameters A, C, and l are updated, where A controls the direction and magnitude of the movement, C introduces stochastic variation, and l defines the spiral trajectory.
8. Hybrid parameter p. The parameter p, with a hybrid deterministic–stochastic formulation, is calculated by combining the current value of a with a random component. Consequently, the distribution of p changes according to the search stage, modifying the relative selection of the encircling-based and spiral update mechanisms (see Equation (17)).
9. Decision based on parameter p. If $p < 0.5$, the whale performs the encircling-based position update; otherwise, it updates its position using the spiral movement around the best feasible solution found. Thus, the value of p determines the update mechanism, while the exploration or exploitation behavior of the encircling mechanism is subsequently determined by the coefficient A.
10. Coefficient vector A. For the encircling-based mechanism, if $|A| < 1$, exploitation is favored, and the whale updates its position based on the best feasible solution, intensifying the search in its neighborhood. If $|A| \geq 1$, a randomly selected search agent is used as the reference to promote global exploration.
11. Update toward the best solution. The whales update their positions with respect to the current best feasible solution, which acts as the prey, according to Equations (6) and (7).
12. Global exploration using a random agent. A random search agent is selected as the reference, and the whales update their positions with respect to this agent to promote exploration of different regions of the constrained solution space, using Equations (13) and (14).
13. Spiral movement. The distance to the best feasible solution is computed, and the position is updated following a spiral trajectory, simulating the whales' attacking behavior (see Equation (11)).
14. Update of the best solution. The best feasible network configuration (G_{best}) is identified together with its corresponding objective-function value (P_{best}). If a new feasible configuration provides a lower active power loss than the current best value, both G_{best} and P_{best} are updated. The improvement of the best solution is also monitored for the stagnation criterion.
15. Iteration increment. The iteration index t is incremented, and the algorithm returns to the iterative cycle until the maximum number of iterations or the stagnation-based stopping criterion is satisfied.
16. Final solution obtained. The final solution G_{best} corresponds to the best feasible radial topology found by AD-BWOA during the optimization process. Its corresponding active power losses and electrical operating variables obtained from DIgSILENT PowerFactory are reported as the final optimization results. This solution represents the best feasible solution obtained under the defined computational procedure and does not imply a mathematical guarantee of global optimality.

The overall optimization procedure, including candidate generation, binary switching-state determination, power-flow evaluation, constraint verification, and updating of the best solution, is illustrated in the flowchart shown in Figure 4.

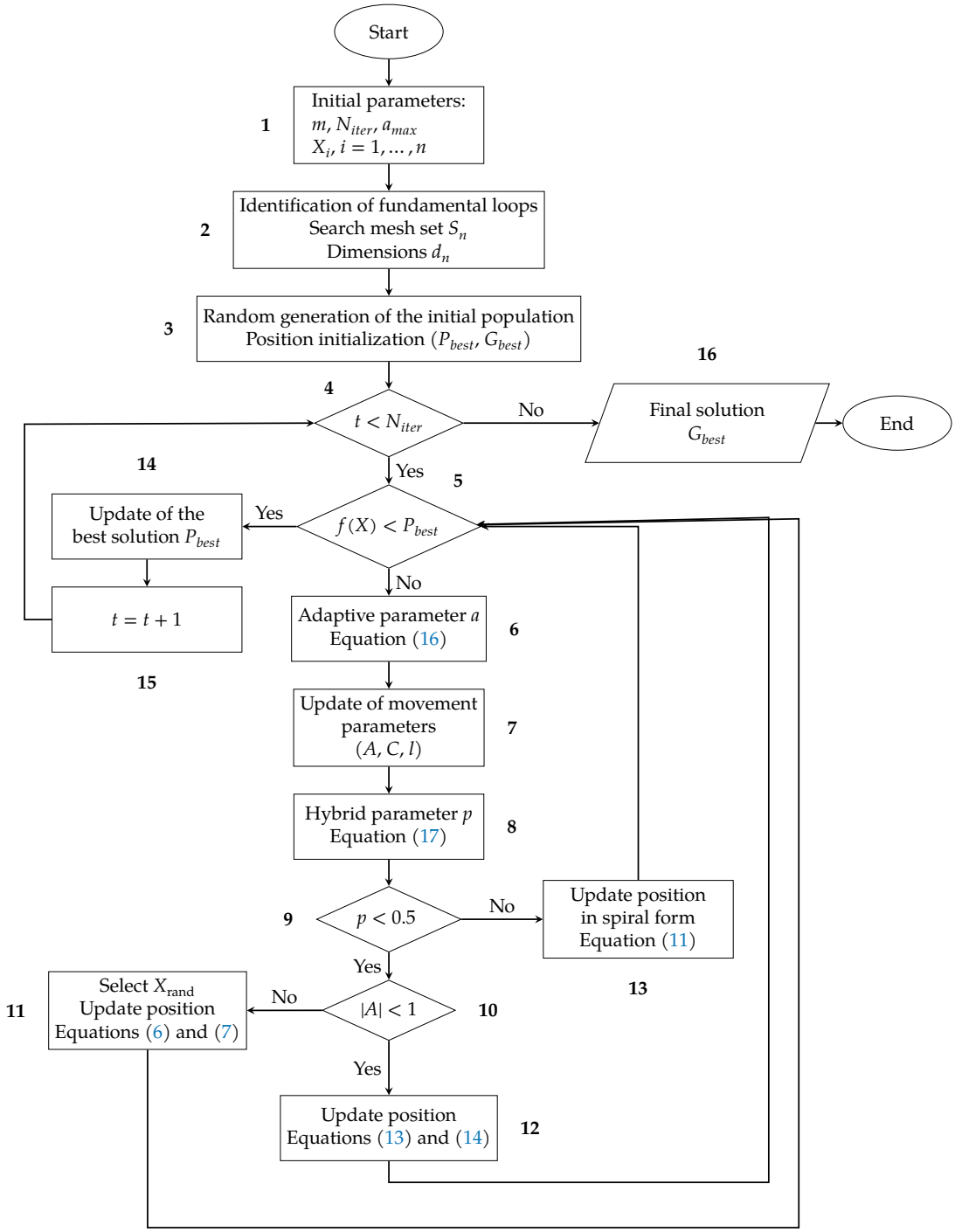


Figure 4. Flowchart of the proposed AD-BWOA method for distribution network reconfiguration.

6. Simulation and Result Analysis

To evaluate the performance of the proposed method for Distribution Network Reconfiguration (DNR), standard IEEE test systems with 69, 94, and 135 buses were analyzed. These benchmark systems are widely adopted in the literature due to their different levels of complexity and scalability, allowing a comprehensive assessment of the algorithm.

The proposed approach, based on the Whale Optimization Algorithm (WOA) with adaptive mechanisms, was implemented in Python and executed on a system equipped with an Intel(R) Core(TM) i7-8650U CPU at 1.90 GHz.

The evaluation focused on convergence behavior, robustness, and computational efficiency. Multiple independent runs were performed to assess the stochastic nature of the

algorithm, considering a population size of m. The analysis included key performance indicators such as active power loss minimization, global optimum recurrence rate, and standard deviation of the obtained solutions.

The simulation parameters (m, N_{iter}, a_{min}, a_{max}, A, C, and NR_m) were defined according to the flowchart shown in Figure 4, ensuring consistent evaluation conditions across all test systems. Electrical simulations were carried out using PowerFactory, where each candidate solution was validated by verifying operational constraints, including voltage limits, current limits, and radiality.

Finally, the parameters A, C, a_{max}, and a_{min} were selected based on recommendations from the literature and empirical sensitivity analysis, ensuring an appropriate balance between exploration and exploitation throughout the optimization process.

6.1. Case Study 1: 69-Bus Distribution System

The 69-bus electrical distribution system, with an apparent power of 10 MVA, proposed by Savier and Das [14], is widely used in the literature for the evaluation and comparison of optimization techniques. The nominal voltage of the system is 12.66 kV, and its structure consists of five fundamental loops.

This system comprises 73 branches equipped with 68 sectionalizing switches and 5 tie switches. Figure 5 illustrates the network topology and its associated loops. Red dashed lines labeled S69 to S73 denote the normally open tie switches, which preserve the radial network configuration. Solid black lines represent energized branches, while horizontal bars indicate the distribution buses and closed sectionalizing switches (S1 to S68). Blue numbers identify the buses, numbered 1 to 69. The gray shaded regions labeled M1 to M5 delineate the five network loops, and the gray circular arrows indicate their respective traversal directions.

Table 2 presents the results obtained for the 69-bus electrical distribution system based on 100 independent simulations, considering a constant value of $K = 5$ and different values of the parameter α, ranging from 0.1 to 1.0 with an increment of 0.1.

Table 2. Results of the 69-Bus electrical distribution system for different values of α (100 simulations).

α	Mean Value (kW)	Std. Dev.	No. of Global Solutions	Best Solution		Worst Solution	
				Losses	Switches	Losses	Switches
0.1	98.319	0.00	100	98.319	[69,14,70,58,61]	98.319	[69,14,70,58,61]
0.2	98.319	0.00	100	98.319	[69,14,70,58,61]	98.319	[69,14,70,58,61]
0.3	98.319	0.00	100	98.319	[69,14,70,58,61]	98.319	[69,14,70,58,61]
0.4	98.319	0.00	100	98.319	[69,14,70,58,61]	98.319	[69,14,70,58,61]
0.5	98.319	0.00	100	98.319	[69,14,70,58,61]	98.319	[69,14,70,58,61]
0.6	98.319	0.00	100	98.319	[69,14,70,58,61]	98.319	[69,14,70,58,61]
0.7	98.319	0.00	100	98.319	[69,14,70,58,61]	98.319	[69,14,70,58,61]
0.8	98.319	0.00	100	98.319	[69,14,70,58,61]	98.319	[69,14,70,58,61]
0.9	98.319	0.00	100	98.319	[69,14,70,58,61]	98.319	[69,14,70,58,61]
1.0	98.319	0.00	100	98.319	[69,14,70,58,61]	98.319	[69,14,70,58,61]

The results show a standard deviation equal to zero for all values of α, indicating a highly consistent convergence behavior of the algorithm, as well as the absence of premature convergence or entrapment in local optima.

The optimal switch configuration obtained was {S69, S14, S70, S58, S61}, achieving a minimum active power loss of 98.319 kW. It can be observed that, for all values of the parameter α, the algorithm converges to the same optimal solution.

However, the values $\alpha = 0.1$ and $\alpha = 0.4$ reached this solution in only 12 iterations, and are therefore considered the most efficient in terms of computational cost and convergence speed.

Table 3 compares the best solution obtained by AD-BWOA with previously reported methods for the 69-bus system.

Figure 6 shows that the proposed method initially exhibits higher power losses than the classical WOA; however, it achieves a rapid reduction in losses during the initial iterations and converges to a solution of approximately 98.319 kW after 12 iterations. In comparison, the classical WOA reaches a similar solution after 27 iterations, indicating a lower iteration count of the proposed method. For $\alpha = 0.4$, the proposed method requires an average simulation time of 99.41 s under the computational platform described above. The legend indicates the number of iterations required to reach convergence for each evaluated method.

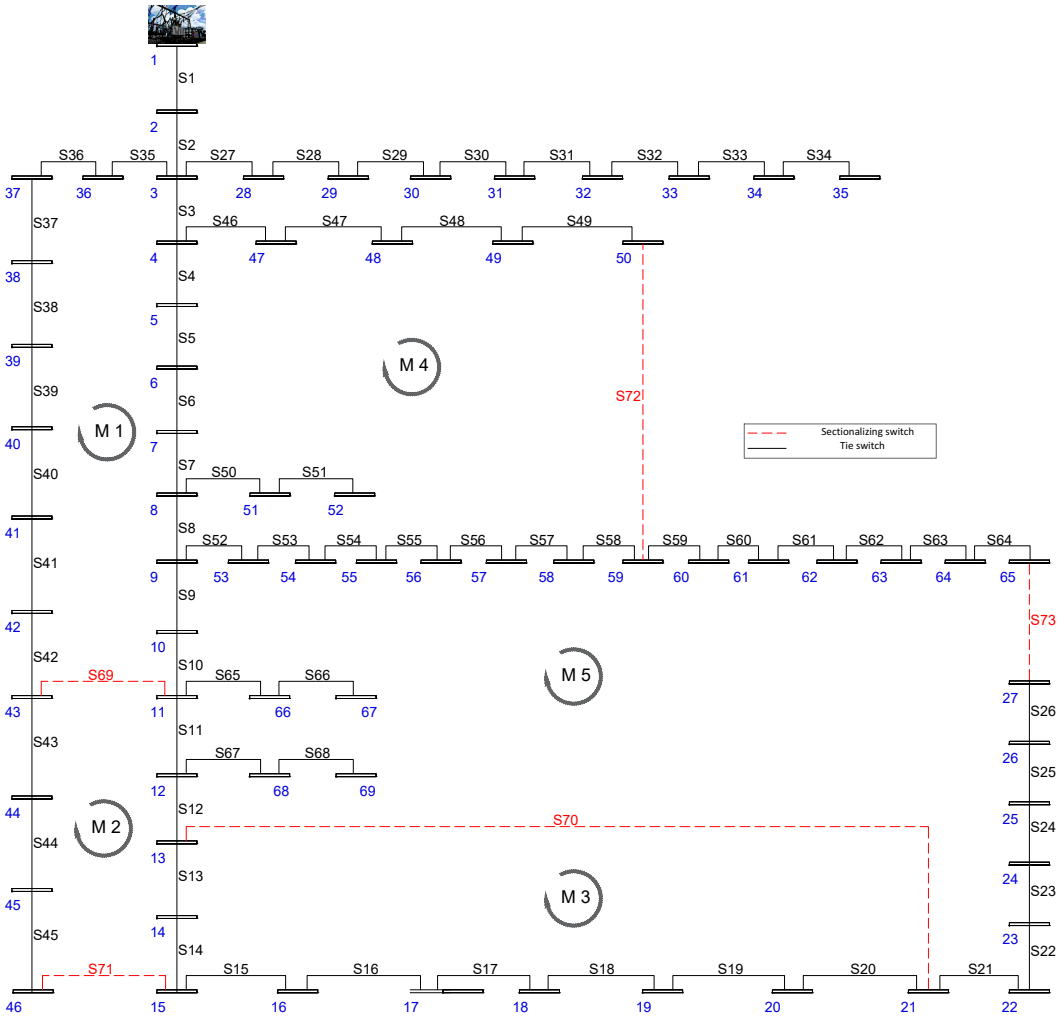


Figure 5. The 69-bus electrical distribution system.

Despite the presence of multiple local optima in the search space, the proposed algorithm consistently obtained high-quality solutions, achieving an active power loss reduction of up to 56.29%. Among the evaluated parameter settings, $N_{\text{iter}} = 100$ and $m = 50$ provides the most favorable trade-off between computational effort and solution quality, with performance comparable to that obtained using larger populations but at a lower computational cost.

Table 3. Comparison of methods for the electrical distribution system.

Method	Open Switches	Losses (kW)	Reduction (%)
AD-BWOA (proposed, $\alpha = 0.1$)	[69,14,70,58,61]	98.319	56.29
WOA [5]	[58,63,14,10,12]	104.860	53.38
IWOA [19]	[69,14,70,58,61]	98.319	56.29
Tabu [20]	[69,14,70,55,61]	98.319	56.29

In the 69-bus system, the initial scenario exhibited a progressive voltage drop along the feeder, reaching a minimum value of 0.909 p.u. at bus 65, with several buses operating close to the lower acceptable limit.

After reconfiguration, the voltage profile improves significantly, increasing the minimum voltage to 0.949 p.u., which represents an approximate recovery of 0.040 p.u. The most significant improvements are observed at the terminal buses (62–65), where voltage increases exceed 0.05 p.u. Overall, a more uniform, stable voltage profile with an improved operational margin is achieved.

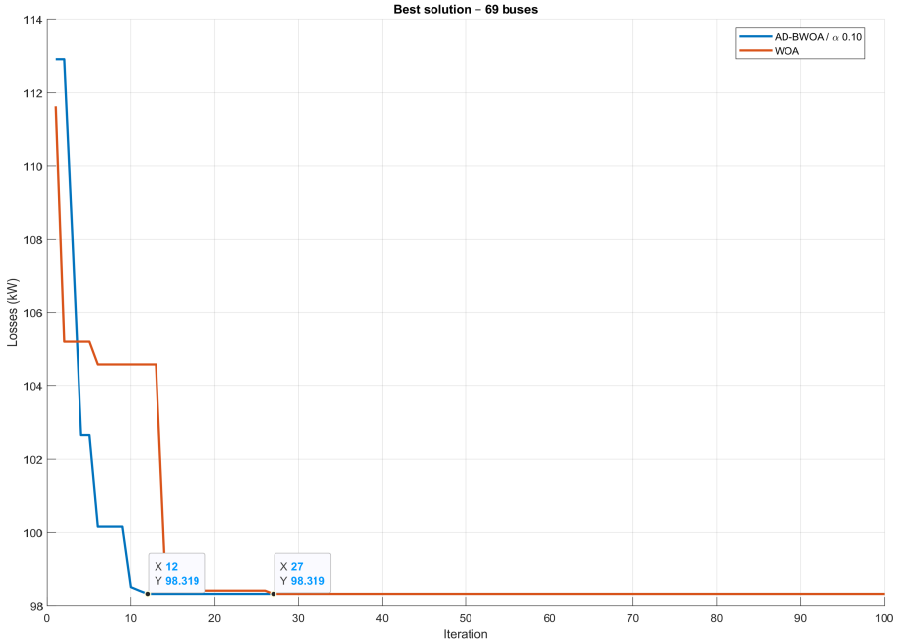


Figure 6. Comparison for the 69-bus electrical distribution system.

6.2. Case Study 2: 94-Bus Distribution System

The 94-bus electrical distribution system, with an apparent power of 100 MVA, proposed by Su and Lee [15], corresponds to a real system from the Taiwan Power Company (TPC) and is widely used as a benchmark for evaluating optimization techniques in distribution networks. The nominal voltage of the system is 11.4 kV, and its topology includes thirteen fundamental loops, which increases the complexity of the reconfiguration problem.

The system comprises 96 branches equipped with 83 sectionalizing switches and 13 tie switches, enabling a wide range of operating configurations subject to the radiality constraint. Figure 7 illustrates the network topology. Red dashed lines labeled S84 to S96 denote the normally open tie switches, which preserve the radial network configuration. Solid black lines represent energized branches, while thick horizontal lines indicate the distribution buses, substation sources (A to K), and closed sectionalizing switches (S1 to S83). Blue numbers identify the buses, numbered 1 to 83. The gray shaded regions labeled M1 to M13 delineate the potential network loops and their associated feeder pairs, while gray circular arrows indicate the traversal direction of each loop.

Table 4 presents the results obtained for the 94-bus system based on 100 independent simulations, considering a constant value of $K = 5$ and different values of the parameter α, ranging from 0.1 to 1.0 with an increment of 0.1. The results show a zero standard deviation for all values of α, indicating highly consistent convergence behavior, as well as the absence of premature convergence or entrapment in local optima.

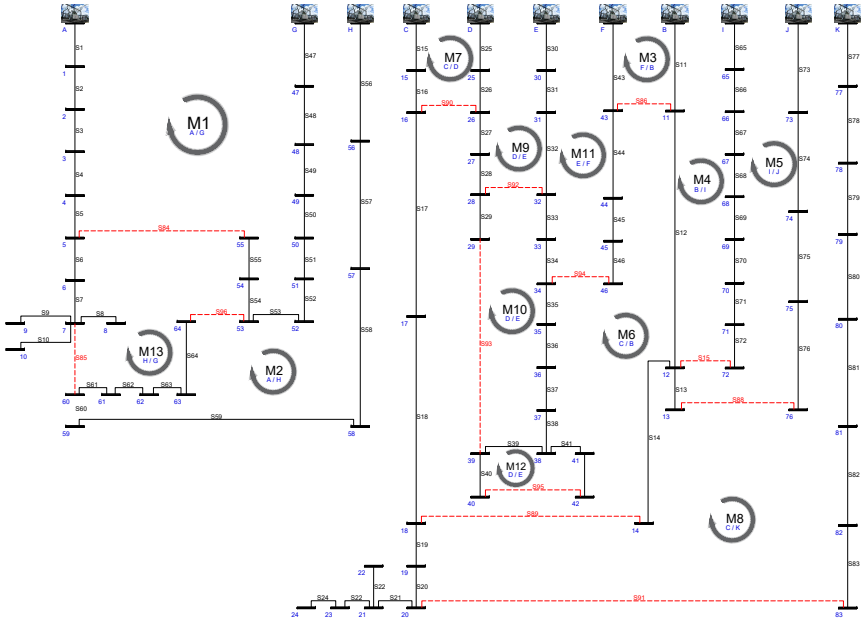


Figure 7. The 94-bus electrical distribution system.

Table 4. Results of the 94-Bus electrical distribution system for different values of α (100 simulations).

α	Mean Value (kW)	Std. Dev.	No. of Global Solutions	Best Solution		Worst Solution	
				Losses	Switches	Losses	Switches
0.1	469.838	0.00	100	469.838	[7,55,86,72,13,89,90,83,92,39,34,42,62]	469.838	[7,55,86,72,13,89,90,83,92,39,34,42,62]
0.2	469.838	0.00	100	469.838	[7,55,86,72,13,89,90,83,92,39,34,42,62]	469.838	[7,55,86,72,13,89,90,83,92,39,34,42,62]
0.3	469.838	0.00	100	469.838	[7,55,86,72,13,89,90,83,92,39,34,42,62]	469.838	[7,55,86,72,13,89,90,83,92,39,34,42,62]
0.4	469.838	0.00	100	469.838	[7,55,86,72,13,89,90,83,92,39,34,42,62]	469.838	[7,55,86,72,13,89,90,83,92,39,34,42,62]
0.5	469.838	0.00	100	469.838	[7,55,86,72,13,89,90,83,92,39,34,42,62]	469.838	[7,55,86,72,13,89,90,83,92,39,34,42,62]
0.6	469.838	0.00	100	469.838	[7,55,86,72,13,89,90,83,92,39,34,42,62]	469.838	[7,55,86,72,13,89,90, 83,92,39,34,42,62]
0.7	470.642	0.00	100	470.642	[7,55,86,72,13,89,90,83,92,39,33,42,62]	470.642	[7,55,86,72,13,89,90, 83,92,39,34,42,62]
0.8	469.838	0.00	100	469.838	[7,55,86,72,13,89,90,83,92,39,34,42,62]	469.838	[7,55,86,72,13,89,90,83,92,39,34,42,62]
0.9	469.838	0.00	100	469.838	[7,55,86,72,13,89,90,83,92,39,34,42,62]	469.838	[7,55,86,72,13,89,90, 83,92,39,34,42,62]
1.0	469.838	0.00	100	469.838	[7,55,86,72,13,89,90,83,92,39,34,42,62]	469.838	[7,55,86,72,13,89,90,83,92,39,34,42,62]

The optimal switch configuration obtained was {S7, S55, S86, S72, S13, S89, S90, S83, S92, S39, S34, S42, S62}, achieving a minimum active power loss of 469.838 kW. It is observed that, for all values of α, the algorithm converges to the same optimal solution.

However, the values $\alpha = 0.2$, $\alpha = 0.3$, and $\alpha = 0.8$ reached this solution in only 21 iterations, and are therefore considered the most efficient in terms of computational cost and convergence speed.

Table 5 compares the best solution obtained by AD-BWOA with previously reported methods for the 94-bus system.

Table 5. Comparison of methods for the 94-bus electrical distribution system.

Method	Open Switches	Active Losses (kW)	Reduction (%)
AD-BWOA (proposed, $\alpha = 0.8$)	[7,55,86,72,88,89,90,83,92,39,34,42,62]	469.838	11.66
BPSO [2]	[7,55,86,72,88,89,90,83,92,39,34,42,62]	469.838	11.66
Tabu [20]	[7,55,86,72,88,89,90,83,92,39,34,42,62]	469.838	11.66

Figure 8 shows that the proposed method initially exhibits higher power losses than the classical WOA; however, it rapidly reduces the losses during the initial iterations and converges to a solution of approximately 98.319 kW after 21 iterations. In comparison, the classical WOA reaches a similar solution after 53 iterations, indicating that the proposed method requires fewer iterations to converge. For $\alpha = 0.8$, the proposed method achieves an average simulation time of 297.16 s, while for $\alpha = 0.3$, the corresponding average simulation time is 299.73 s. For the two parameter settings that reached the reported solution in 21 iterations, the average simulation times were 297.16 s for $\alpha = 0.8$ and 299.73 s for $\alpha = 0.3$, showing that identical iteration counts do not necessarily imply identical execution times.

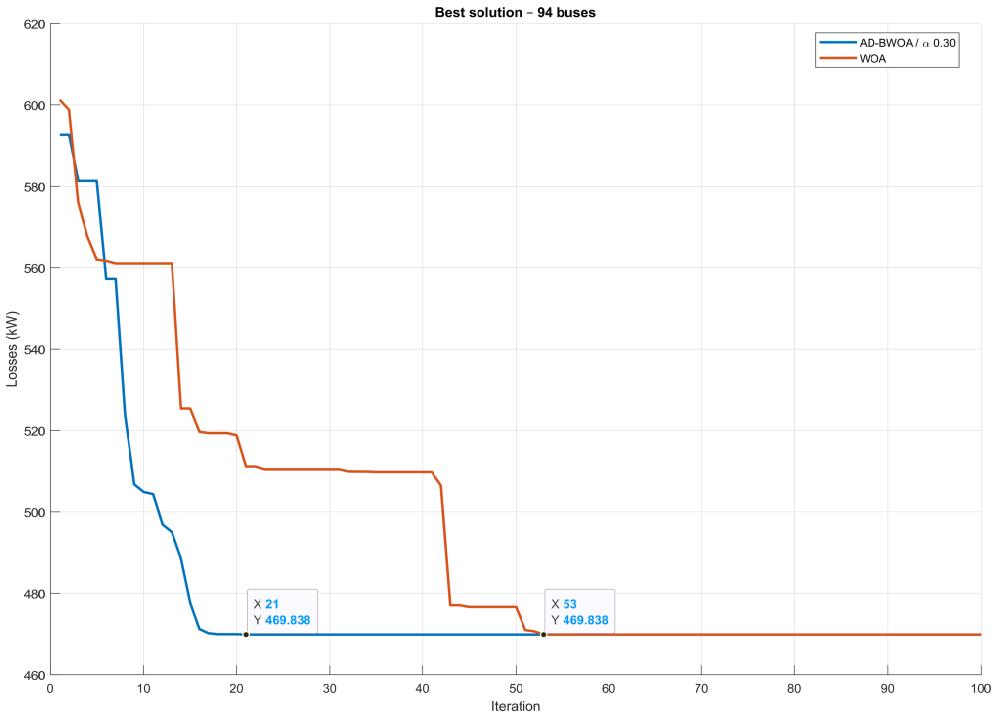


Figure 8. Comparison for the 94-bus electrical distribution system.

The algorithm achieved the global optimum in more than 11.66% of the runs, despite the presence of multiple local optima. The most favorable configuration in terms of computational cost–performance trade-off corresponds to $N_{\text{iter}} = 100$ and $m = 80$.

In the 94-bus system, the base case exhibited multiple voltage drop regions along the feeder, with a minimum value of 0.9286 p.u., particularly in the initial buses and at the feeder end.

After optimization, the minimum voltage increases to approximately 0.953 p.u., eliminating critical undervoltage conditions. The most significant improvements occur in the initial buses (3–10), with increases close to 0.03 p.u., as well as in the final section (78–83). Overall, the reconfiguration reduces voltage profile dispersion and improves global voltage regulation.

6.3. Case Study 3: 135-Bus Distribution System

The 135-bus electrical distribution system, with an apparent power of 100 MVA, proposed by Mantovani, Casari, and Romero [16], corresponds to a real distribution system and is widely used in the literature for the evaluation and comparison of optimization techniques applied to distribution networks. The nominal voltage of the system is 13.8 kV, and its topology consists of twenty-one fundamental loops, which increases the complexity of the reconfiguration problem.

The system comprises 156 branches equipped with 135 sectionalizing switches and 21 tie switches, enabling a wide range of operating configurations subject to the radiality constraint. Figure 9 illustrates the network topology and its associated loops. Red dashed lines labeled S136 to S156 denote the normally open tie switches, which preserve the radial network configuration. Solid black lines represent energized branches, while thick horizontal lines indicate the distribution buses, substation sources, and closed sectionalizing switches (S1 to S135). Blue numbers identify the buses, numbered 1 to 223. The gray shaded regions labeled M1 to M21 delineate the potential network loops, while gray circular arrows indicate the traversal direction of each loop.

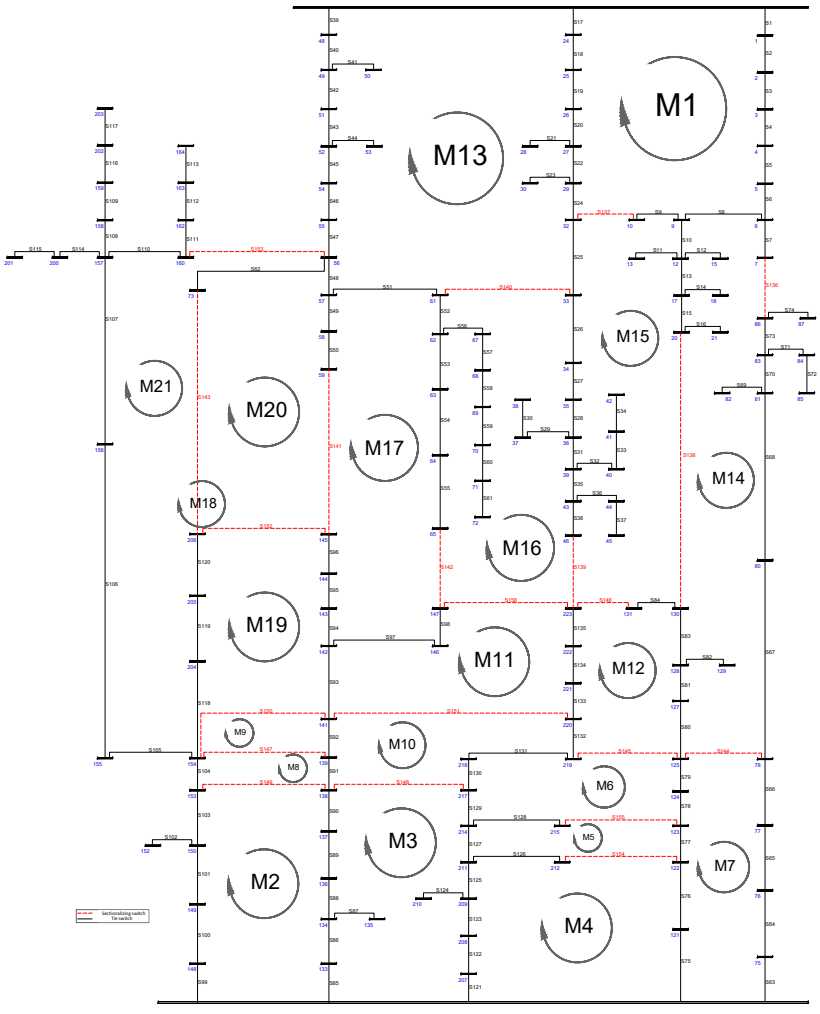


Figure 9. The 135-bus electrical distribution system.

Table 6 presents the results obtained for the 135-bus distribution system based on 100 independent simulations, considering a constant value of $K = 5$ and different values of the parameter α. The values of α are concentrated around 0.8, where more favorable solutions are obtained.

Table 6. Results of the 135-Bus electrical distribution system for different values of α (100 simulations).

α	Average Time (s)	Mean Value (kW)	Std. Dev.	No. of Runs Reaching the Reported Best Solution	Best Solution		Worst Solution	
					Losses	Switches	Losses	Switches
0.75	-	279.889	0.00	100	279.889	[137,90,148,126,128,145,144 ,147,150,151,156,84,51,7 ,138,139,53,118,96,141,106]	279.889	[137,90,148,126,128,145,144 ,147,150,151,156,84,51,7 ,138,139,53,118,96,141,106]
0.76	1049.11	279.858	0.00	100	279.858	[137,90,148,126,128,145,144 ,147,150,151,156,84,51,7 ,138,139,53,118,96,141,106]	279.858	[137,90,148,126,128,145,144 ,147,150,151,156,84,51,7 ,138,139,53,118,96,141,106]
0.77	1008.82	279.858	0.00	100	279.858	[137,90,148,126,155,145,144 ,147,150,151,135,146,51,7 ,138,35,142,118,96,141,106]	279.858	[137,90,148,126,155,145,144 ,147,150,151,135,146,51,7 ,138,35,142,118,96,141,106]
0.78	-	281.664	0.00	100	281.664	[137,149,148,126,128,145,144 ,147,150,151,156,84,51,7 ,138,139,53,119,96,141,106]	281.664	[137,149,148,126,128,145,144 ,147,150,151,156,84,51,7 ,138,139,53,119,96,141,106]
0.79	1025.42	279.858	0.00	100	279.858	[137,90,148,126,155,145,144 ,147,150,151,135,146,51,7 ,138,35,142,118,96,141,106]	279.858	[137,90,148,126,155,145,144 ,147,150,151,135,146,51,7 ,138,35,142,118,96,141,106]
0.80	575.73	279.858	0.00	100	279.858	[137,90,148,126,155,145,144 ,147,150,151,135,146,51,7 ,138,35,142,118,96,141,106]	279.858	[137,90,148,126,155,145,144 ,147,150,151,135,146,51,7 ,138,35,142,118,96,141,106]
0.81	-	279.889	0.00	100	279.889	[137,90,148,126,128,145,144 ,147,150,151,156,84,51,7 ,138,139,53,118,96,141,106]	279.889	[137,90,148,126,128,145,144 ,147,150,151,156,84,51,7 ,138,139,53,118,96,141,106]
0.82	-	280.728	0.00	100	280.728	[137,90,148,126,128,145,144 ,147,150,151,135,84,51,7 ,138,38,54,119,96,141,106]	280.728	[137,90,148,126,128,145,144 ,147,150,151,135,84,51,7 ,138,38,54,119,96,141,106]
0.83	-	280.748	0.00	100	280.748	[137,90,148,126,128,145,144 ,147,150,151,135,84,51,7 ,138,38,53,119,95,141,106]	280.748	[137,90,148,126,128,145,144 ,147,150,151,135,84,51,7 ,138,38,53,119,95,141,106]

Table 6. *Cont.*

α	Average Time (s)	Mean Value (kW)	Std. Dev.	No. of Runs Reaching the Reported Best Solution	Best Solution		Worst Solution	
					Losses	Switches	Losses	Switches
0.84	1033.850	279.858	0.00	100	279.858	[137,90,148,126,155,145,144 ,147,150,151,135,146,51,7 ,138,35,142,118,96,141,106]	279.858	[137,90,148,126,155,145,144 ,147,150,151,135,146,51,7 ,138,35,142,118,96,141,106]
0.85	-	279.889	0.00	100	279.889	[137,90,148,126,128,145,144 ,147,150,151,156,84,51,7 ,138,139,53,118,96,141,106]	279.889	[137,90,148,126,128,145,144 ,147,150,151,156,84,51,7 ,138,139,53,118,96,141,106]
0.86	-	280.265	0.00	100	280.265	[137,90,148,126,128,145,144 ,147,150,151,135,84,51,7 ,138,38,53,118,95,141,106]	280.265	[137,90,148,126,128,145,144 ,147,150,151,135,84,51,7 ,138,38,53,118,95,141,106]
0.87	-	284.253	0.00	100	284.253	[9,149,148,126,128,145,144 ,147,150,151,135,84,140,7 ,138,139,54,143,96,141,106]	284.253	[9,149,148,126,128,145,144 ,147,150,151,135,84,140,7 ,138,139,54,143,96,141,106]
0.88	-	280.042	0.00	100	280.042	[137,90,148,126,128,145,144 ,147,150,151,135,84,51,7 ,138,38,54,118,96,141,106]	280.042	[137,90,148,126,128,145,144 ,147,150,151,135,84,51,7 ,138,38,54,118,96,141,106]
0.89	-	280.597	0.00	100	280.597	[137,90,148,126,155,145,144 ,147,150,151,156,146,51,7 ,138,38,53,119,96,141,106]	280.597	[137,90,148,126,155,145,144 ,147,150,151,156,146,51,7 ,138,38,53,119,96,141,106]
0.90	1018.57	279.858	0.00	100	279.858	[137,90,148,126,155,145,144 ,147,150,151,135,146,51,7 ,138,35,142,118,96,141,106]	279.858	[137,90,148,126,155,145,144 ,147,150,151,135,146,51,7 ,138,35,142,118,96,141,106]
0.91	-	279.889	0.00	100	279.889	[137,90,148,126,128,145,144 ,147,150,151,156,84,51,7 ,138,139,53,118,96,141,106]	279.889	[137,90,148,126,128,145,144 ,147,150,151,156,84,51,7 ,138,139,53,118,96,141,106]
0.92	-	280.029	0.00	100	280.029	[137,90,148,126,155,145,144 ,147,150,151,135,146,51,7 ,138,35,55,118,95,141,106]	280.029	[137,90,148,126,155,145,144 ,147,150,151,135,146,51,7 ,138,35,55,118,95,141,106]

Table 6. *Cont.*

α	Average Time (s)	Mean Value (kW)	Std. Dev.	No. of Runs Reaching the Reported Best Solution	Best Solution		Worst Solution	
					Losses	Switches	Losses	Switches
0.93	-	280.748	0.00	100	280.748	[137,90,148,126,128,145,144 ,147,150,151,135,84,51,7 ,138,38,53,119,95,141,106]	280.748	[137,90,148,126,128,145,144 ,147,150,151,135,84,51,7 ,138,38,53,119,95,141,106]
0.94	-	280.380	0.00	100	280.380	[137,90,148,126,155,145,144 ,147,150,151,135,146,51,7 ,138,35,142,119,95,141,106]	280.380	[137,90,148,126,155,145,144 ,147,150,151,135,146,51,7 ,138,35,142,119,95,141,106]
0.95	-	280.748	0.00	100	280.748	[137,90,148,126,128,145,144 ,147,150,151,135,84,51,7 ,138,38,53,119,95,141,106]	280.748	[137,90,148,126,128,145,144 ,147,150,151,135,84,51,7 ,138,38,53,119,95,141,106]
0.96	1044.79	279.858	0.00	100	279.858	[137,90,148,126,155,145,144 ,147,150,151,135,146,51,7 ,138,35,142,118,96,141,106]	279.858	[137,90,148,126,155,145,144 ,147,150,151,135,146,51,7 ,138,35,142,118,96,141,106]

The results show a zero standard deviation for all values of α, indicating a highly consistent convergence behavior of the algorithm, as well as the absence of premature convergence or entrapment in local optima.

The optimal switch configuration obtained was {S137, S90, S148, S126, S155, S145, S144, S147, S150, S151, S135, S146, S51, S7, S138, S35, S142, S118, S96, S141, S106}, achieving a minimum active power loss of 279.858 kW. It is observed that, for all values of the parameter α, the algorithm converges to a near-optimal solution. However, the value $\alpha = 0.8$ reaches this solution in only 37 iterations and is therefore considered the most efficient in terms of computational cost and convergence speed.

Table 7 summarizes the best solution obtained by AD-BWOA for the 135-bus system. Because directly comparable published results under equivalent computational settings were not available for all performance indicators considered here, no controlled superiority claim is made for this case.

Table 7. Comparison of methods for the 135-bus electrical distribution system.

Method	Open Switches	Active Losses (kW)	Reduction (%)
AD-BWOA (proposed)	[137,90,148,126,155, 145,144,147,150,151, 135,146,51,7,138, 35,142,118,96,141,106]	279.858	12.5

Figure 10 shows that the proposed method initially exhibits higher power losses than the classical WOA; however, it achieves a rapid reduction in losses during the initial iterations and converges to a solution of approximately 279.858 kW after 37 iterations. In comparison, the classical WOA reaches a similar solution after 82 iterations, indicating a lower iteration count of the proposed method. For $\alpha = 0.8$, the reported solution was reached after 37 iterations with an average simulation time of 575.73 s. The legend indicates the number of iterations required to reach convergence for each evaluated method.

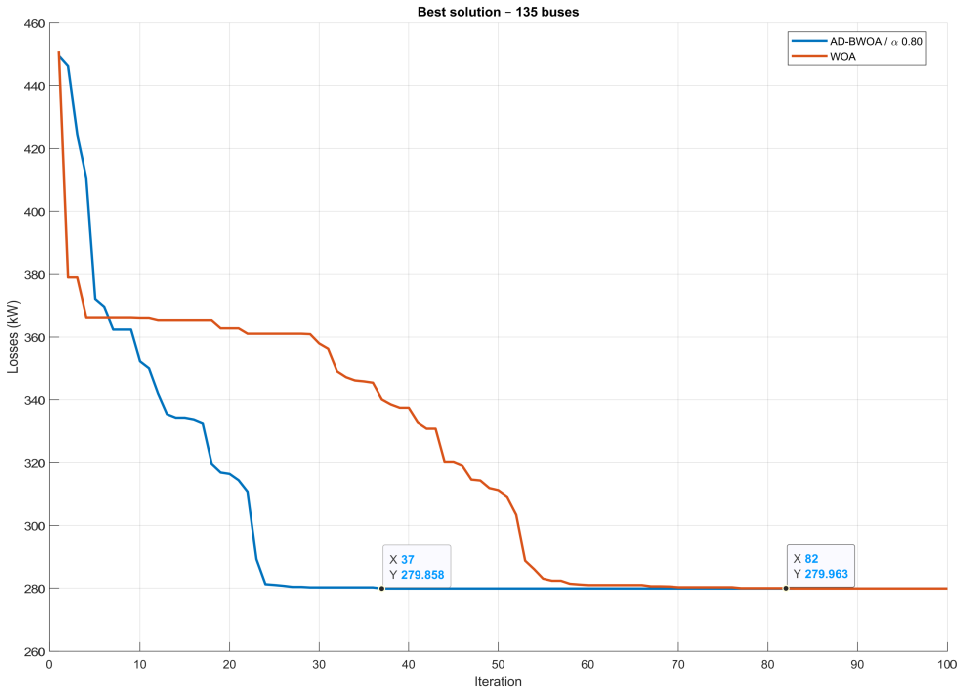


Figure 10. Comparison for the 135-bus electrical distribution system.

The optimization process is consistent and robust. The algorithm achieved the global optimum in more than 12.5% of the runs, despite the presence of multiple local optima. The most favorable configuration in terms of computational cost–performance trade-off corresponds to $N_{\text{iter}} = 100$ and $m = 120$, as it provides results comparable to those obtained with larger populations while requiring lower computational effort.

In the 135-bus system, although most of the network operated within acceptable limits, a critical region was identified between buses 42 and 58, where the minimum voltage reached 0.9313 p.u.

After reconfiguration, the minimum voltage increases to approximately 0.966 p.u., with improvements on the order of 0.03–0.035 p.u. in the most critical region. The final voltage profile is more uniform and stable, eliminating the most severe voltage drops and increasing the operational margin of the system.

7. Conclusions

This paper presented an Adaptive Dynamic Binary Whale Optimization Algorithm (AD-BWOA) for solving the Distribution Network Reconfiguration (DNR) problem, with the objective of minimizing active power losses while satisfying electrical and topological operating constraints. The proposed method extends the conventional Whale Optimization Algorithm (WOA) by combining a nonlinear adaptation of the convergence parameter with an adaptive deterministic–stochastic position-update mechanism. These modifications are designed to improve the balance between exploration and exploitation throughout the search process, thereby enhancing convergence behavior and solution consistency.

The performance of the proposed algorithm was evaluated on 69-, 94-, and 135-bus distribution systems through multiple independent runs. The results show that AD-BWOA consistently obtains high-quality solutions comparable to the best or reference solutions reported for the evaluated systems. In particular, the 69- and 94-bus cases exhibited high repeatability under the tested conditions, with consistent switching configurations across the independent runs. The algorithm also showed favorable convergence behavior, while the stagnation-based stopping criterion reduced unnecessary iterations once no further improvement in the best solution was observed. For the larger 135-bus system, AD-BWOA remained capable of obtaining competitive solutions despite the increased search-space complexity and number of switching alternatives.

From an operational perspective, the reconfigured network configurations resulted in relevant reductions in active power losses and improvements in voltage profiles while satisfying the established operating constraints. These results indicate that the solutions obtained by AD-BWOA can contribute to improving the efficiency and operating conditions of radial distribution systems, particularly by reducing losses and mitigating voltage deviations in more critical portions of the network.

The proposed approach is currently limited to a single-objective DNR formulation focused on active power loss minimization and does not explicitly consider other relevant operational aspects, such as reliability indices, switching costs, distributed generation, renewable-energy variability, or time-varying demand. Future work will therefore extend AD-BWOA to multi-objective formulations incorporating these factors and investigate its scalability in larger distribution systems. The stagnation-based stopping criterion may also be adapted to multi-objective problems by considering the evolution of the Pareto front, while uncertainties associated with distributed generation and demand can be addressed through scenario-based or stochastic formulations. In addition, a controlled component-wise ablation study will be conducted to quantify the marginal contributions of the coupled adaptive *a*-*p* mechanism, the fundamental-loop-based search-space reduction, the binary discretization procedure, and the stagnation-based stopping criterion using appropriately

redefined algorithmic variants. Further studies will also investigate the applicability of the proposed method to real-time or near-real-time smart-grid operation.

Author Contributions: Conceptualization, A.G.P., D.Z.Ñ.H., F.J.S.P., J.L.d.N., J.P.B.R. and Y.P.M.R.; methodology, A.G.P., F.J.S.P., J.L.d.N., J.P.B.R. and Y.P.M.R.; software, J.L.d.N. validation, J.L.d.N., J.P.B.R., Y.P.M.R., A.G.P. and D.Z.Ñ.H.; formal analysis, A.G.P., J.L.d.N. and Y.P.M.R.; investigation, A.G.P. and J.L.d.N.; resources, Y.P.M.R.; data curation, A.G.P. ; writing—original draft preparation, A.G.P.; writing—review and editing, J.L.d.N., Y.P.M.R., A.G.P. and D.Z.Ñ.H.; visualization, A.G.P.; supervision, Y.P.M.R.; project administration, Y.P.M.R. All authors have read and agreed to the published version of the manuscript.

Funding: This research received no external funding.

Institutional Review Board Statement: Not applicable.

Informed Consent Statement: Not applicable.

Data Availability Statement: The compact raw results, derived analysis tables, parameter documentation, network models, and execution and analysis scripts needed to reproduce the reported summaries are provided with the article's/reproducibility files. The complete per-evaluation trace collection is available from the corresponding author because of its file size.

Acknowledgments: The authors gratefully acknowledge the Vice-Rectorate for Research and the Faculty of Electrical Engineering at Universidad Nacional de Ingeniería (Lima, Peru), as well as the Department of Electrical Engineering at the Federal University of Paraíba (Brazil), for their institutional support and collaboration throughout the development of this work. The authors reviewed and edited the output and take full responsibility for the content of this publication.

Conflicts of Interest: The authors declare no conflicts of interest.

References

1. Dehghany, N.; Asghari, R. Multi-objective optimal reconfiguration of distribution networks using a novel meta-heuristic algorithm. *Int. J. Electr. Comput. Eng.* **2024**, *14*, 3557–3569. [CrossRef]
2. Pegado, R.; Naupari, Z.; Molina, Y.; Castillo, C. Radial Distribution Network Reconfiguration for Power Losses Reduction Based on Improved Selective BPSO. *Electr. Power Syst. Res.* **2019**, *169*, 206–213. [CrossRef]
3. Nguyen, T.T.; Nguyen, T.T.; Le, B. Optimization of Electric Distribution Network Configuration for Power Loss Reduction Based on Enhanced Binary Cuckoo Search Algorithm. *Comput. Electr. Eng.* **2021**, *90*, 106893. [CrossRef]
4. Kahouli, O.; Alsaif, H.; Bouteraa, Y.; Ben Ali, N.; Chaabene, M. Power System Reconfiguration in Distribution Network for Improving Reliability Using Genetic Algorithm and Particle Swarm Optimization. *Appl. Sci.* **2021**, *11*, 3092. [CrossRef]
5. Solanki, A.; Mehroliya, S.; Arya, A.; Tomar, S.; Nikum, K. Reconfiguration of the Distribution Network Using a Whale Optimization Algorithm. In Proceedings of the 2023 IEEE International Students' Conference on Electrical, Electronics and Computer Science (SCEECS), Bhopal, India, 18–19 February 2023. [CrossRef]
6. Alqahtani, M.; Marimuthu, P.; Moorthy, V.; Pangedaiah, B.; Reddy, C.R.; Kiran Kumar, M.; Khalid, M. Investigation and Minimization of Power Loss in Radial Distribution Network Using Gray Wolf Optimization. *Energies* **2023**, *16*, 4571. [CrossRef]
7. Wu, Y.; Liu, J.; Wang, L.; An, Y.; Zhang, X. Distribution Network Reconfiguration Using Chaotic Particle Swarm Chicken Swarm Fusion Optimization Algorithm. *Energies* **2023**, *16*, 7185. [CrossRef]
8. Siregar, Y.; Tambun, T.S.J.; Panjaitan, S.P.; Tanjung, K.; Yana, S. Distribution Network Reconfiguration Utilizing the Particle Swarm Optimization Algorithm and Exhaustive Search Methods. *Bull. Electr. Eng. Inform.* **2024**, *13*, 821–831. [CrossRef]
9. Jia, H.; Zhu, X.; Cao, W. Distribution Network Reconfiguration Based on an Improved Arithmetic Optimization Algorithm. *Energies* **2024**, *17*, 1969. [CrossRef]
10. Enacheanu, B.; Raison, B.; Caire, R.; Devaux, O.; Bienia, W.; HadjSaid, N. Radial network reconfiguration using genetic algorithm based on the matroid theory. *IEEE Trans. Power Syst.* **2008**, *23*, 186–195. [CrossRef]
11. Lavorato, M.; Franco, J.F.; Rider, M.J.; Romero, R. Imposing Radiality Constraints in Distribution System Optimization Problems. *IEEE Trans. Power Syst.* **2011**, *27*, 172–180. [CrossRef]
12. Mirjalili, S.; Lewis, A. The Whale Optimization Algorithm. *Adv. Eng. Softw.* **2016**, *95*, 51–67. [CrossRef]
13. Sun, G.; Shang, Y.; Yuan, K.; Gao, H. An Improved Whale Optimization Algorithm Based on Nonlinear Parameters and Feedback Mechanism. *Int. J. Comput. Intell. Syst.* **2022**, *15*, 38. [CrossRef]

14. Savier, J.S.; Das, D. Impact of Network Reconfiguration on Loss Allocation of Radial Distribution Systems. *IEEE Trans. Power Deliv.* **2007**, *22*, 2473–2480. [CrossRef]
15. Su, C.; Lee, C. Network Reconfiguration of Distribution Systems Using Improved Mixed-Integer Hybrid Differential Evolution. *IEEE Trans. Power Deliv.* **2003**, *18*, 1022–1027. [CrossRef]
16. Mantovani, J.R.S.; Casari, F.; Romero, R.A. Reconfiguração de sistemas de distribuição radiais utilizando o critério de queda de tensão. *SBA Controle Autom.* **2000**, *11*, 150–159.
17. Pereira, F.S.; Vittori, K.; Da Costa, G.R.M. Distribution System Reconfiguration for Loss Reduction Based on Ant Colony Behavior. In Proceedings of the IEEE/PES Transmission and Distribution Conference and Exposition: Latin America, Caracas, Venezuela, 15–18 August 2006; pp. 1–5. [CrossRef]
18. Cardero Cardero, E.; Salazar Fonseca, I.; Castro Torres, N.A.; García, D.J.; Cervantes Oliva, J.; Barrero Formigo, D.d.R. Reconfiguración multiobjetivo en sistemas de distribución primaria con presencia de generación distribuida. *Ingeniare. Rev. Chil. Ing.* **2022**, *30*, 592–601. [CrossRef]
19. Ali, E.S.; Elazim, S.M.A. Optimal Network Reconfiguration via Improved Whale Optimization Approach. *Wseas Trans. Power Syst.* **2023**, *18*, 141–151. [CrossRef]
20. Pinheiro Filho, L.O. Reconfiguração de Redes de Distribuição Utilizando Algoritmo de Busca Tabu. Master's Thesis, Universidade Federal da Paraíba, João Pessoa , Brasil, 2022.

Disclaimer/Publisher's Note: The statements, opinions and data contained in all publications are solely those of the individual author(s) and contributor(s) and not of MDPI and/or the editor(s). MDPI and/or the editor(s) disclaim responsibility for any injury to people or property resulting from any ideas, methods, instructions or products referred to in the content.